Structure and Morphology of the Aliphatic Polyester Poly-β-propiolactone in Solution-Grown Chain-Folded Lamellar Crystals

Yukiko Furuhashi, Tadahisa Iwata, Pawel Sikorski,‡ Edward Atkins,†,‡ and Yoshiharu Doi*

Polymer Chemistry Laboratory, RIKEN Institute, Hirosawa, Wako-shi, Saitama 351-0198, Japan

Received June 20, 2000; Revised Manuscript Received October 16, 2000

ABSTRACT: Solution-grown, chain-folded lamellar crystals of poly-β-propiolactone (PPL) have been crystallized isothermally from cyclohexanone at 55 °C. The lathlike crystals have been studied by transmission electron microscopy (imaging and diffraction), atomic force microscopy, and X-ray diffraction. A new crystal structure, the γ-structure, has been discovered. Using the experimental diffraction data and computerized modeling the structure has been refined, including the detailed geometry of the adjacent re-entry folds. The chain is in an all-trans or 1-fold helix conformation and the structure consists of a two-chain, C-faced, orthorhombic unit cell with the following parameters: $a = 0.700 \pm 0.002$ nm, $b = 0.490 \pm 0.002$ nm, and c (chain axis) $= 0.493 \pm 0.002$ nm. The setting angles, with respect to the a axis, are $\pm 51.5°$ for the corner and center chains, respectively. The lamellae are 5 nm in thickness and the chains run orthogonal to the lamellar surface, although there is evidence for slight c-axis shearing of the chain-folded sheets. The general fold direction is along the a axis (long axis of the crystal) and the chain folds successively in the (110) and ($1\bar{1}0$) planes. Comparisons are made with previous structures for PPL fibers and related chain-folded polymers.

Introduction

Aliphatic polyesters are currently of interest because of their biodegradability.[1−3] Recent activity in this laboratory, concerned with the structure and morphology of solution-grown chain-folded lamellar crystals prepared from aliphatic polyesters, has emanated from related studies on the microbially produced polyesters: poly[(*R*)-3-hydroxybutyrate] (P(3HB)) and its copolymers,[4,5] polymers which are sources for biodegradable plastics.[6] As a natural development of our studies, we have investigated the aliphatic polyester poly-β-propiolactone (PPL), a polymer which has two methylene units sandwiched between successive ester groups, as illustrated in the following formula: $[-CH_2-CH_2-CO-O-]_n$. PPL might be considered to represent the backbone structure of P(3HB), since P(3HB) has a methyl side group: $[-CH(CH_3)-CH_2-CO-O-]_n$. Thus, comparison of the structures and morphologies of the two structures is of particular interest. At this point, it is convenient to note that the PPL chain is directionally specific: a feature of importance later when considering chain-folded lamellar structures in detail.

In this contribution, we describe how the PPL polyester can be isothermally crystallized from solution in the form of chain-folded lamellae and present our results and interpretations concerning the structure and morphology of the lamellar crystals, using electron microscopy, both imaging and diffraction, together with both wide- and small-angle X-ray diffraction obtained from sedimenting lamellae into oriented mats. We will be particularly interested in the relationship between the straight-stem crystallography and the folding behavior.

This research venture was undertaken to study the nature of the crystalline chain-folded lamellae from PPL, since to our knowledge, no previous detailed work has been reported. We will also take the opportunity to compare our findings with previous results reported for PPL fibers[7,8] and to consider the relationship of PPL lamellae to chain-folded lamellae structures reported for other members of the aliphatic polyester family, and in addition, the related polyamides and polyethylene.

Previous Structural Studies. Two different chain conformations and crystal structures (α- and β-structures)[7,8] have been proposed for PPL, based on X-ray diffraction patterns obtained from oriented fibers, and the salient features are as follows.

α-Structure. The chain conformation is purported to be a 2-fold helix with a chain axis (c) repeat of 0.702 nm,[7] thus, an advance per monomer of 0.702/2 = 0.351 nm. This latter value is 26% less than that expected for the all-trans planar structure[8] and Wasai et al.[7] suggested that the chain conformation was axially compressed in some fashion but did not offer any detailed model.

***β*-Structure.** The characteristic feature of the X-ray diffraction pattern, obtained from cold-drawn fibers, is continuous diffraction streaking on all layer lines, other than the equator ($l = 0$), where discrete diffraction signals are observed.[7,8] Thus, the chains have no axial register, and the structure resembles a liquid crystalline nematic. The layer line periodicity of 0.477 nm spacing[8] is close to that of the fully extended, all-trans, planar chain conformation, as shown in Figure 1a. The formal description of the chain conformation is a 1-fold helix. The discrete equatorial diffraction signals index on the rectangular net and therefore the unit cell can be classified as a C-faced centered orthorhombic, with the following parameters:[8] $a = 0.773$ nm, $b = 0.448$ nm, and c (chain axis) $= 0.477$ nm. The projection of the proposed structure parallel to the c axis is shown in Figure 1b; the all-trans planar chains lie within the ac plane to form sheets.[8] A small-angle meridional diffraction signal was recorded at a spacing of 7.6 nm, for cold drawn fiber

* To whom all correspondence should be addressed. Telephone: +81-48-467-9402. Fax: +81-48-462-4667.
† RIKEN Visiting Eminent Scientist.
‡ Permanent Address: H. H. Wills Physics Laboratory, University of Bristol, Tyndall Avenue, Bristol BS8 1TL, UK.

10.1021/ma001070t CCC: $19.00
Published on Web 11/16/2000

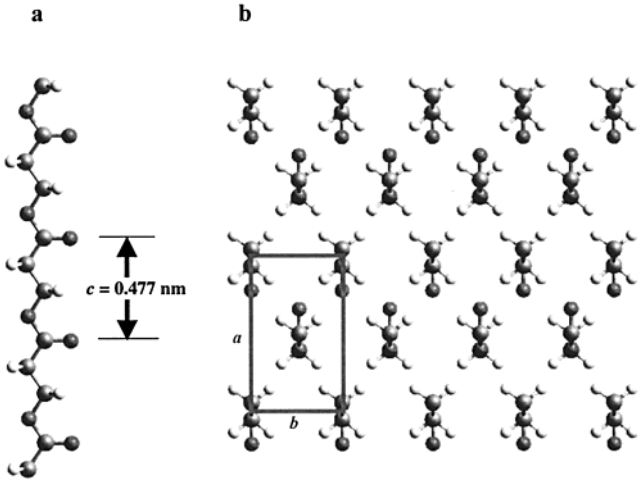

Figure 1. PPL β-structure proposed by Suehiro et al.[8] (a) Projection of the all-trans PPL $[-CH_2-CH_2-CO-O-]_n$ chain in ball-and-stick mode. The all-trans chain periodicity was reported[8] to be 0.477 nm. (b) View parallel to the *c* axis showing the 0° setting angle of the chains with respect to the *a* axis.

samples which (*sic*) might reflect a lamellar structure. The noticeable layer line streaking was thought to be caused by the lack of *c*-axis correlation between neighboring chains in structure, but any consequences this might have for chain folding were not discussed.

Structure of P(3HB). The crystal structures of drawn fibers of both the optically active and racemic forms have been reported.[9−11] The unit cell is orthorhombic with the following unit cell parameters:[9] a = 0.576 nm, b = 1.320 nm, and c (chain axis) = 0.596 nm. The chain conformation is a 2-fold helix of type ($\bar{G}\bar{G}TT$) with left-handed chirality and the space group is $P2_12_12_1$.

Experimental Section

Materials. An original PPL sample (weight-average molecular weight (M_w) = 367 000 and polydispersity (DPI) = 2.2) was kindly supplied by Tokuyama Corp. The sample was purified by precipitation in methanol from a chloroform solution and dried in an oven at 35 °C. To obtain both lower molecular weight and polydispersity (M_w = 70 000 and DPI = 1.6) for preparation of solution-grown lamellar crystals, the original PPL was treated by 1 N aqueous KOH alkali-hydrolysis with 18-crown-6-ether, according to the method reported previously.[4] The purified PPL (50 mg) was dissolved in chloroform (6 mL). After addtion of 40 mg of 18-crown-6 ether to the PPL solution, the mixture was stirred for 2.5 h at 35 °C. The phase-separated organic layer was pipetted into a sample tube and dried over anhydrous magnesium sulfate. After filtration, the organic layer was precipitated into methanol.

Preparation of Crystalline Lamellae. An isothermal crystallization procedure was adopted for preparing the chain-folded lamellae. Cyclohexanone (normal laboratory grade) was found best for the solution-grown lamellar crystals. A 0.025 wt % solution of PPL was prepared at 70 °C and maintained for 1 h in a silicone oil bath. The solution was allowed to cool to 55 °C and held at that temperature for 36 h before allowing it to cool to room temperature.

Transmission Electron Microscopy. Drops of the crystal suspension were placed on carbon-coated transmission electron microscopy (TEM) grids and allowed to dry. Some samples were shadowed with Pt−Pd alloy to enhance the contrast of the TEM images. To calibrate the electron diffraction patterns, some crystals were mounted on carbon-coated grids sputtered with gold. All calibration was achieved at room temperature. Samples were tilted up to 45° in order to record other electron diffraction zones. Individual lamella were surface-decorated by evaporating polyethylene under vacuum conditions, according to the method of Wittmann and Lotz[12] followed by shadowing with Pt−Pd alloy. TEM images and electron diffraction patterns were observed at room temperature using a JEM-2000FX II electron microscope operating at 120 kV and recorded using Kodak 4489 and SO-163 films, respectively.

Atomic Force Microscopy. Drops of the crystal suspension were placed on freshly cleaved mica and allowed to dry. The thickness and surface morphology of the chain-folded lamellar crystals were examined using atomic force microscopy (AFM) using a SPI3700/SPA300 (Seiko Instruments Inc.). Pyramid-shaped Si_3N_4 tips, mounted on 100 μm long microcantilevers, each with a spring constant of 0.09 N/m, were used for the contact mode experiments. Simultaneous registration was performed in the contact mode for height and deflection images.

X-ray Diffraction. Oriented crystal mats suitable for X-ray diffraction were prepared by sucking the crystal suspension through a 0.1 μm PTFE filter using a water aspirator. The wide-angle X-ray diffraction patterns were obtained at room temperature using nickel-filtered Cu Kα radiation of wavelength 0.1541 nm, from a Rigaku D-9C sealed beam X-ray generator operating at 40 kV and 35 mA. The X-ray diffraction patterns were recorded using a point-collimated beam and a flat-plate film holder. Calcium fluoride (d_{111} = 0.3154 nm) was dusted onto selected samples for calibration purposes. Small-angle X-ray diffraction patterns were obtained with nickel-filtered Cu Kα from a Philips sealed beam generator operating at 35 kV and 40 mA. In this case a point-collimated beam and a long evacuated flat-plate camera were used to reduce air scatter. In each case the beam was directed parallel to the surface of the mat, and the mat normal was vertical.

Model Building and Analyses of Structure. The software package Cerius2, version 3.8 (MSI), was used in the structural modeling and diffraction simulations. The basic strategy was to determine the molecular conformation of the PPL chain and the molecular packing arrangement within the unit cell. After the initial model building stage, a combination of energy minimization (EMin), using the CVFF force field, and simulations of diffraction patterns was used. This ensured that the model was stereochemically sound and that the simulated diffraction patterns were in good agreement with the experimental data. In the computer-simulated X-ray diffraction patterns, the degree of arcing and intensity were chosen to match the experimental X-ray diffraction patterns as closely as possible.

Modeling the Folds. At the stage where the structure of the lamellar crystalline core was established, the adjacent reentry folding geometry was modeled. Two different folds, (1) placing the ester unit close to the apex of the hairpin turn and (2) placing the dimethylene alkane segment centrally in the fold, were considered. In each case, the straight-stems were connected by appropriate chain fragments and the energy of the fold minimized. The constraints on the straight-stem segments close to the fold were then relaxed so that the total number of atoms needed to form a stress-free fold could be established.

Results

PPL Lamellar Crystals. Figure 2a shows PPL lamellar crystals grown from cyclohexanone solution. The crystals are tapered, lathlike lamellae. The lamellae have dimensions 0.5−1.5 μm in width and 5−8 μm in length. To determine the orientation of the crystal axis, triple-exposure experiments on the PPL lamellar crystals were performed. The selected electron diffraction pattern (a beam normal to the lamellar surface) is shown as an inset in the correct azimuthal orientation. This shows that the crystallographic *a* axis lies along the long axis of the crystal and the *c* axis projected unit cell is orthogonal.

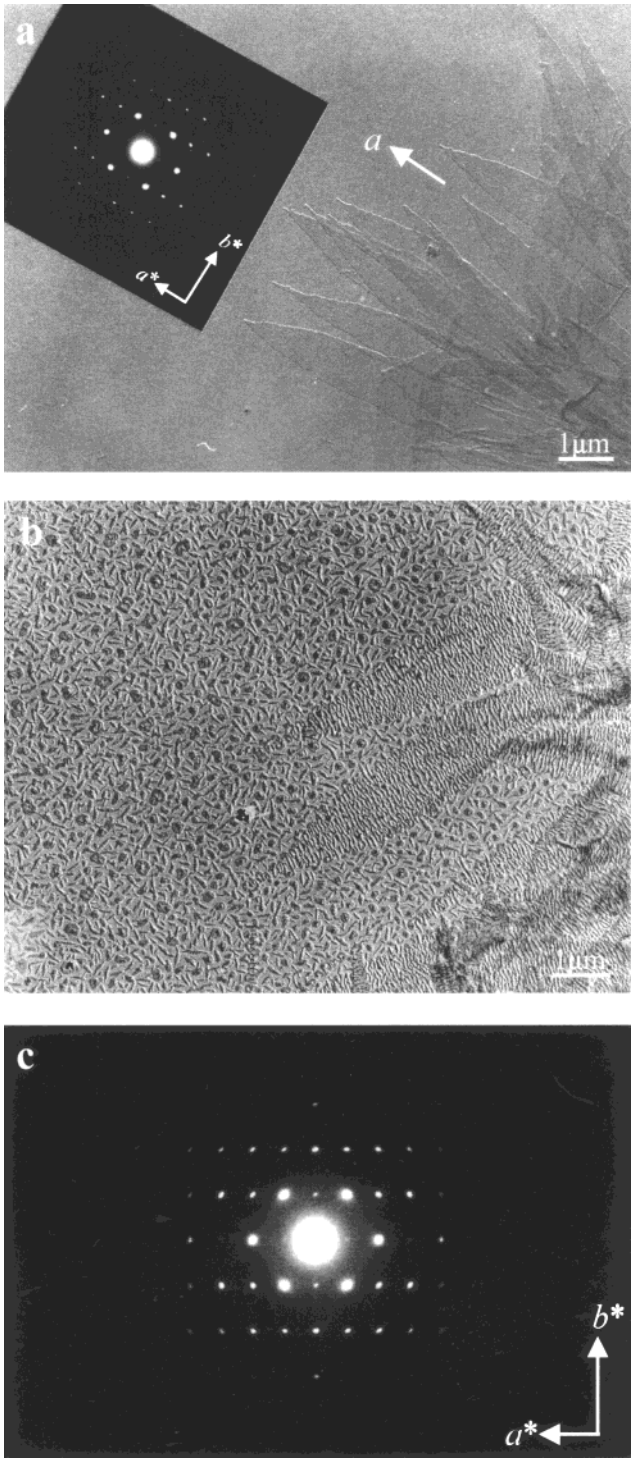

Figure 2. (a) Transmission electron micrograph of the PPL chain-folded lamellar crystals shadowed with Pt−Pd to enhance the contrast. The tapered, lathlike lamellae are 0.5−1.5 μm in width and 5−8 μm in length. The *hk*0 electron diffraction inset is at the correct azimuthal orientation and shows that the *a** axis is parallel to the long axis (*a* axis) of the crystals. (b) PPL lamellar crystals decorated with polyethylene. (c) Selected area (*hk*0) electron diffraction taken with the beam normal to the lamellar surface. The diffraction signals index on a rectangular net with $a^* = 1.420$ nm^{-1} and $b^* = 2.045$ nm^{-1}. The strong {110} family suggests the cell is C-faced centered.

Figure 2b shows the PPL lamellar crystals decorated with polyethylene. The polyethylene rods are relatively well-ordered orthogonal to the long axis of the lamellar crystals. Thus, the general direction of chain-folding occurs along the long axis of the lamellar crystals. Since no sectorization is observed in these polyethylene decorated PPL crystals, the chain-folding is directionally constant over the whole lamellar surface.

In certain cases, noticeable striations are observed running parallel to the long axis of the crystals, as shown in Figure 3a. Figure 3b shows a computer-generated Fourier transform of this image. Three distinct orientations are seen, relating to the three crystal orientations in Figure 3a. In each case, a peak is observed at a distance corresponding to a spacing of 15 nm, confirming that the striations occur regularly. We believe that these striations are caused by twinning, involving small (approximately a few degrees) *c* axis shear in the *b* direction (see Figure 3c). Sometimes these corrugations can collapse as illustrated in Figure 3d.

Figure 4a shows the AFM image of the PPL lamellar crystal. The height profile trace estimates the crystal thickness to be 5.0 ± 0.2 nm (see Figure 4b). The average contour length of our PPL chains is 250 nm and therefore the molecular chains of PPL must be folded within the lamella.

Diffraction Study. The electron diffraction pattern taken with the beam normal to the mat surface is displayed in Figure 2c and the diffraction signals lie on a rectangular net. We believe this diffraction pattern is the weighted *hk*0 reciprocal lattice. Upon calibration of the electron diffraction pattern, all the electron diffraction spots can be indexed in terms of orthogonal reciprocal lattice with the following parameters: $a^* = 1.420$ nm^{-1}, $b^* = 2.045$ nm^{-1}, and $\gamma^* = 90°$. The sample was also rotated in order to search for *hkl* diffraction signals that could provide an estimate of the *c* parameter. The electron diffraction data from tilted samples, helped by the X-ray diffraction results from oriented mats, where the incident beam is orthogonal to the chain axis, enabled the unit cell *c* parameter to be ascertained and estimated. The electron diffraction spacings, together with estimated intensities, are listed in Table 1a. They index on an orthorhombic unit cell with the following parameters: $a = 0.700$ nm; $b = 0.490$ nm; *c* (chain axis) = 0.493 nm.

The wide-angle X-ray diffraction pattern obtained from an oriented mat is shown in Figure 5a and the measured diffraction spacings are listed in Table 1b. The equatorial diffraction signals (*hk*0) index on a rectangular net with $a = 0.700$ nm and $b = 0.490$ nm. These values are the same, within experimental error, as the results obtained from the electron diffraction *hk*0 reciprocal plane from an individual lamella. A very weak equatorial diffraction signal is noticed at 1.40 nm, a value twice the *a* parameter. We do not have a watertight explanation for the occurrence of this rather weak diffraction signal. Interestingly, medium-angle equatorial X-ray diffraction signals with superlattice values have previously been reported for other chain-folded polyester lamellar crystals, and a rippling nature to the fold surface was offered as a possibility.[13] A meridional diffraction signal occurs at a spacing of 0.493 nm and other *hkl* diffraction signals indicate that they lie on a layer line with this spacing. Figure 5b is a schematic diagram giving the indices of the prominent diffraction signals and showing the weaker diffraction arcs. The layer line spacing of 0.493 nm[14] is slightly larger than that of reported[8] for PPL β-structure model, although both have an all-trans chain conformation. On the basis

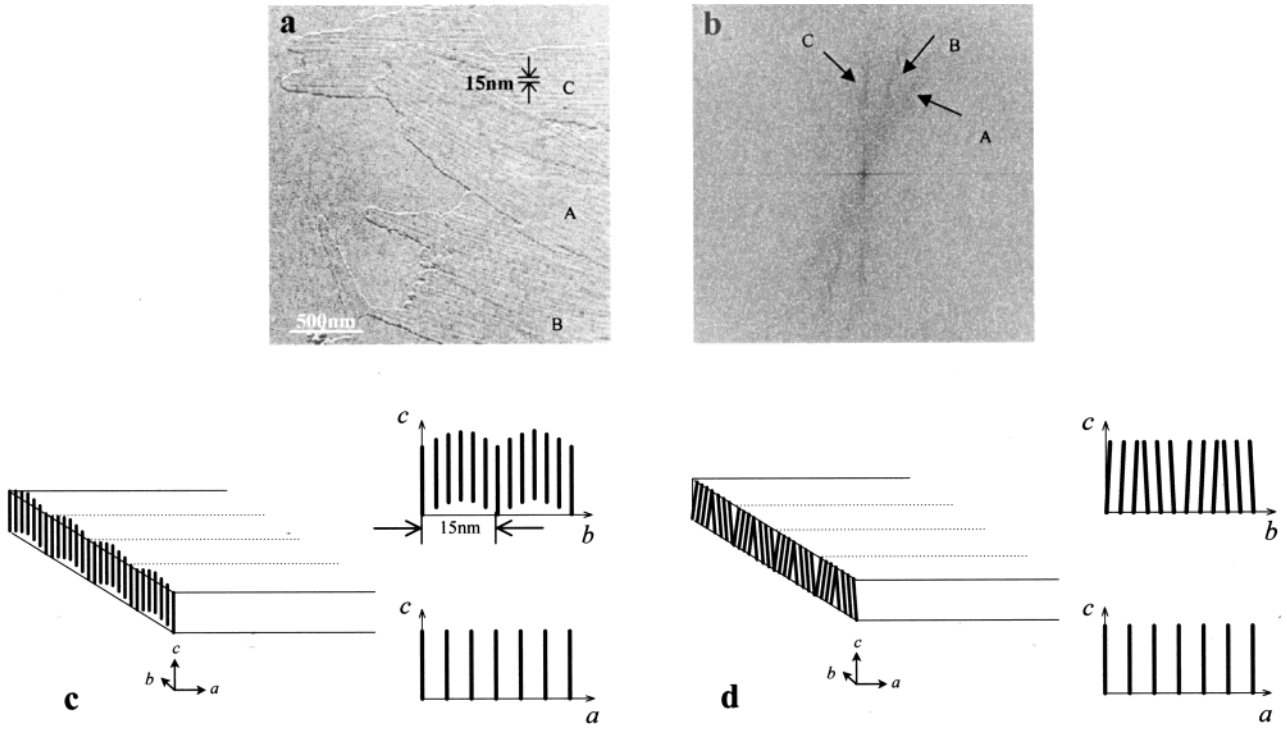

Figure 3. (a) TEM image showing striations running parallel to the long axis of PPL crystals, oriented in three different directions. (b) Computer-generated Fourier transform of part a. In each case, a peak (arrowed) is observed at a spacing corresponding to 15 nm, confirming that the striations are periodic. (c and d) Two models proposed for these striations.

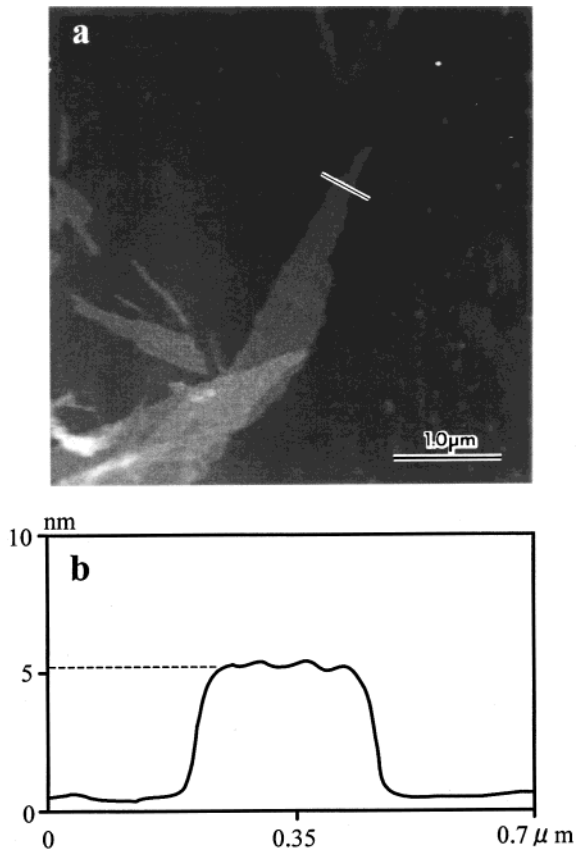

Figure 4. (a) AFM image of PPL crystal. (b) Height profile trace along line indicated in part a.

of the X-ray diffraction pattern combined with the electron diffraction diagram, an orthorhombic unit cell was determined with the following parameters: $a = 0.700 \pm 0.002$ nm; $b = 0.490 \pm 0.002$ nm; c (chain axis) $= 0.493 \pm 0.002$ nm.

The strong 110 diffraction signal, in both the X-ray and electron diffraction patterns, suggests that the unit cell is C-faced centered. The calculated density based on two chain segments passing through the basal *ab* plane is 1.42 g cm^{-3}. For chain-folded crystals of PPL, a molecule that has chain polarity, a minimum of two-chain segments per unit cell is also a necessary condition. In the low-angle diffraction region a meridional diffraction signal is observed at a spacing of 5.12 ± 0.05 nm (see Figure 5c), together with its second order. We believe these peaks are orders of the lamellar stacking periodicity (LSP) in the sedimented mat. The value matches that of the estimated 5 nm for the thickness of a single lamella in the AFM experiments.

Structure Modeling and Refinement

Lamellar Core Crystal Structure. The diffraction evidence favors an all-trans, 1-fold helix, chain conformation similar to that reported[8] for PPL β-structure fibers (see Figure 6a). The stereochemical parameters are given in Table 2a.

Although the chain conformation and density of the crystalline core of our PPL chain-folded lamellar crystals matches that of the β-structure fibers, comparison of the rectangular *ab* basal plane highlights substantial differences in the chain packing organization; our *a* value is 10% smaller, and our *b* value is 9% greater. Accurate stereochemical packing calculations, coupled with matching of the intensity values,[15] of both X-ray and electron diffraction patterns, using Cerius computer-simulated patterns, show that the chain packing is different from the previously reported β-structure found in cold-drawn fibers.[8] Figure 6b shows views of the crystal structure lattice parallel to the *c* axis of the refined crystal structure. The relative setting angles of the corner and center chains with respect to the *a* axis are $\pm$ 51.5°, respectively. Changes in these angles by ~1° create

Table 1. Comparison of Observed and Calculated Diffraction Spacings

(a) Electron Diffraction Spacings from PPL Lamellar Crystals

hkl[a]	d_{obsd} (nm)	d_{calcd} (nm)	int_{obsd}[b]	hkl[a]	d_{obsd} (nm)	d_{calcd} (nm)	int_{obsd}[b]
layer line zero							
010	0.491	0.490	m	030	0.163	0.163	m
110	0.402	0.401	vs	230	0.148	0.148	w
200	0.353	0.350	vs	420	0.143	0.142	w
210	0.285	0.285	s	510	0.136	0.135	vw
020	0.246	0.245	m	330	0.131	0.131	m
120	0.231	0.231	m	430	0.210	0.119	m
310	0.212	0.211	s	600	0.117	0.117	vw
220	0.201	0.201	m	240	0.115	0.116	w
400	0.176	0.175	w				
320	0.170	0.169	m	first layer line			
410	0.166	0.165	vw	201[c]	0.291	0.285	m

(b) X-ray Diffraction Spacings from Oriented, Sedimented PPL Lamellar Crystals

hkl[d]	d_{obsd} (nm)[e]	d_{calcd} (nm)	int_{obsd}[b]	hkl[d]	d_{obsd} (nm)[e]	d_{calcd} (nm)	int_{obsd}[b]
LSP				200	0.348 E	0.350	s
1st order	5.12 M	5.12	vs	210	0.283 E	0.285	s
2nd order	2.46 M	2.56	m	120	0.231 E	0.231	m
				310	0.210 E	0.211	w
superlattice	1.40 E	double a-value	vw	220	0.200 E	0.201	vw
100	0.700 E	0.700	w	001	0.493 M	0.493	m
110	0.403 E	0.401	vs	002	0.246 M	0.247	m

[a] Indexed on an orthorhombic unit cell with parameters $a = 0.700 \pm 0.002$ nm, $b = 0.490 \pm 0.002$ nm, and c (chain axis) $= 0.493 \pm 0.002$ nm. [b] Key: vs, very strong; s, strong; m, medium; w, weak, vw, very weak. [c] From tilted ED experiments. [d] Indexed on an orthorhombic unit cell with parameters $a = 0.700 \pm 0.002$ nm, $b = 0.490 \pm 0.002$ nm, and c (chain axis) $= 0.493 \pm 0.002$ nm. [e] E: equatorial. M: meridional.

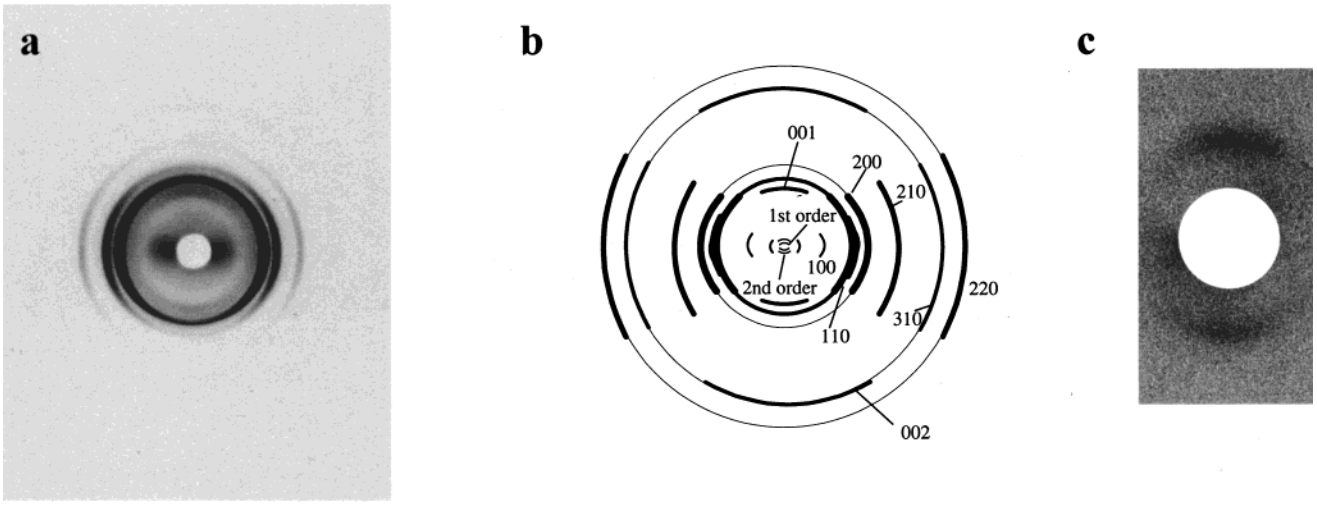

Figure 5. (a) Wide-angle X-ray diffraction pattern from oriented, sedimented mats of PPL; incident beam parallel to mat surface and mat normal vertical. (b) Schematic diagram of X-ray pattern showing the weaker arcs and providing the indices for the prominent diffraction signals. (c) Low-angle diffraction pattern showing the first order of the LSP meridional diffraction signal at a spacing of 5.12 ± 0.05 nm.

serious interatomic clashes; not too surprising in view of the relatively high density of these crystals (1.42 g cm^{-3}). Thus, accurate stereochemical packing calculations, coupled with the optimum matching of the calculated and experimental diffraction intensities using Cerius software, show that the crystalline core of the PPL chain-folded lamellae is substantially different from any previously reported model. It seems logical to refer to this new crystalline phase as the γ-structure. We hasten to add that we do not believe that this new crystal structure is a consequence of chain-folding since unpublished work from this laboratory on nonfolded PPL oligoamides give the same unit cell dimensions.

The calculated weighted reciprocal $hk0$ lattice,[15] shown in Figure 7a, matches the equivalent experimental pattern obtained from an individual lamellar crystal in Figure 2c. The computer simulated X-ray diffraction pattern is shown in Figure 7b[16] can be compared with the experimental X-ray diffraction pattern shown in Figure 5a. Figure 8a provides a view of the structure approximately parallel to the b axis in order to visualize the relative c-axis displacement of the center with respect to the corner chains within the straight-stem or crystalline core structure. Figure 8b is an oblique view of the lamellar core crystal structure.

Chain Folding. We know from the polyethylene decoration results (see Figure 2b) that the predominant direction of the chain folding is parallel to the a axis, i.e., along the long axis of the crystals. However, we also know that the chains must fold along the (110) and (1$\bar{1}$0) planes, via the straight-stems running up and down through the chain-folded crystalline core, i.e., from corner to center and back to corner chain as illustrated in Figure 6b. This folding mechanism is similar to that

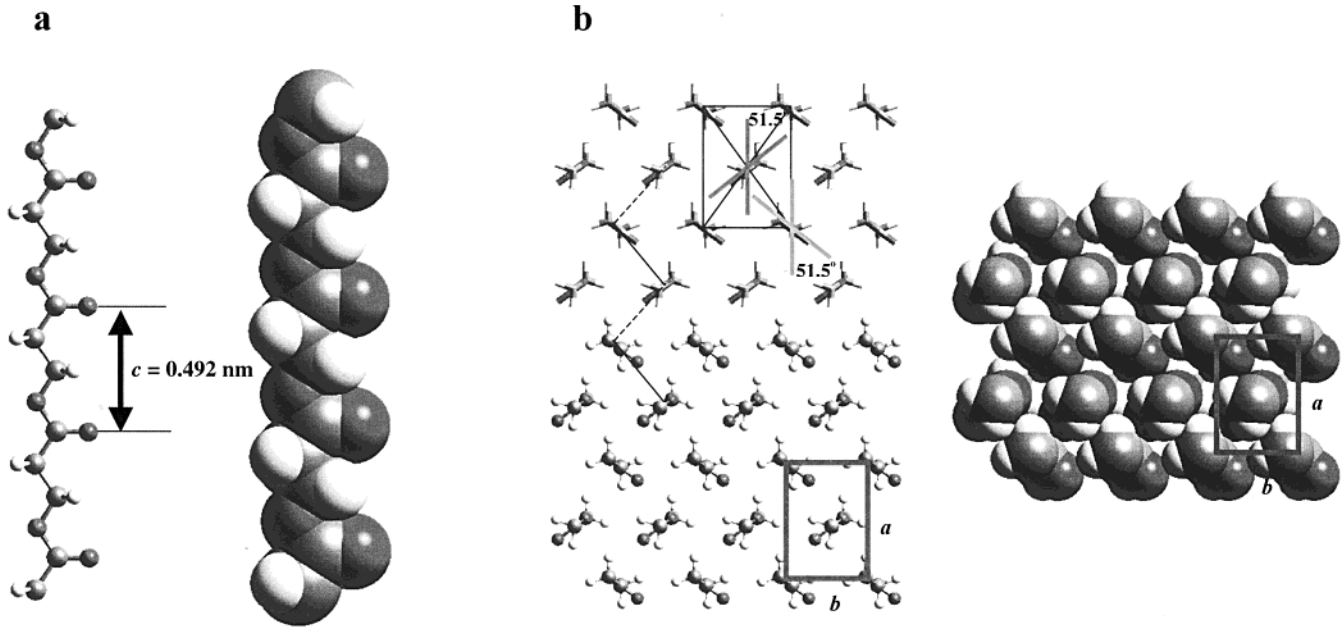

Figure 6. (a) Computer-generated model of the PPL all-trans conformation in both ball-and-stick (left) and space-filling mode (right). The computer-refined conformation has a *c*-repeat of 0.492 nm, the same as the value of 0.493 ± 0.002 nm measured experimentally. (b) Views of the PPL crystal structure, parallel to the *c* axis, that best match the experimental diffraction data; the boxes represent the unit cell. The chain setting angles, with respect to the *a* axis, of the corner and center chains are ±51.5°, respectively. In the stick/ball-and-stick model on the left, the diagonal continuous and dashed lines represent the folding direction, top and bottom of the crystal, respectively. The equivalent space-filling model on the right illustrates how well the molecules pack together.

Table 2. Stereochemical Parameters

(a) For the All-Trans Conformation[a]

bond lengths (nm)		bond angles (deg)		torsion angles (deg)	
C_I-C_{II}	0.153	$C_I-C_{II}-C_{III}$	112	$C_I-C_{II}-C_{III}-O_I$	178
$C_{II}-C_{III}$	0.153	$C_{II}-C_{III}-O_I$	113	$C_{II}-C_{III}-O_I-C_I$	−177
$C_{III}-O_I$	0.139	$C_{III}-O_I-C_I$	114	$C_{III}-O_I-C_I-C_{II}$	178
O_I-C_I	0.145	$O_I-C_I-C_{II}$	114	$O_I-C_I-C_{II}-C_{III}$	−177
$C_{III}=O$	0.124	$C_{II}-C_{III}=O$	122	$C_I-C_{II}-C_{III}=O$	−3
		$O=C_{III}-O_I$	125	$O=C_{III}-O_I-C_I$	1

(b) For the Fold

bond no.[b]	bond type	torsion angles (deg)	bond no.[b]	bond type	torsion angles (deg)
1	$C_{II}-C_I$	172	6	C_I-O_I	−174
2	C_I-O_I	−178	7	O_I-C_{III}	171
3	O_I-C_{III}	160	8	$C_{III}-C_{II}$	2
4	$C_{III}-C_{II}$	−90	9	$C_{II}-C_I$	180
5	$C_{II}-C_I$	42	10	C_I-O_I	−178

[a] $[-C_I-C_{II}-C_{III}-O_I-]C_I$ (with C_{III} double-bonded to O)

[b] See Figure 9.

reported for P(3HB) chain-folded crystals.[17] A computer modeling exercise of PPL reveals that ester units need to be incorporated within the hairpin turn; the dimethylene alkane segments are far too short to span the diagonal distance of 0.425 nm between the antiparallel chains in the crystalline core.

Nature of the Folds. Energy minimization of adjacent re-entry folds, involving the appropriate stereochemical criteria were performed. The best fold is shown in Figure 9a. The dimethylene segment is close to the fold center and straddled by two ester units. A fold placing an ester unit centrally in the hairpin turn (see Figure 9b) was less satisfactory. The restricted torsional rotation about the O−CO bond frustrates this latter fold conformation. Thus, the fold geometry shown in Figure 9a was chosen for the final structure. The stereochemical parameters are given in Table 2b.

Chain-Folded Lamellar Structure. Figure 10a shows a view of the lamellar surface (orthogonal to the *c* axis) of the complete chain-folded lamella. It should be noted in passing that there are two possible packing modes for adjacent folds. Figure 10a shows the chain-folded lamellar structure with the folds out of phase; they may also fold in phase. Geil[18] has previously discussed this aspect when considering chain-folding in polyethylene crystals. In our case, these two possibilities do not influence the straight-stem crystal structure and are energetically equivalent. The chain-folded lamellae must pack within the LSP of 5.12 nm, and allowing for the fold geometry shown in Figure 9 results in straight-stems containing nine repeating monomers. The maximum outer-limit thickness of the crystalline lamellar is 5.08 nm; just less than the measured lamellar stacking periodicity of 5.12 nm. Figure 10b shows an oblique view of the complete adjacent re-entry folded lamellar crystal. For the molecular weight used, the chain end defects would on average occur every 100 chain segments, or ≅20 nm.

Discussion

Within the general context of polymeric structures it is useful to compare facets of this new PPL γ-structure with related chain-folded structures.

Comparison with Polyethylene. The all-trans conformation of the PPL chain resembles that of polyethylene (PE).[18−20] The usual crystal structure of chain-folded PE is a C-face centered orthorhombic, with the basal (*ab* plane) rectangular net and having a basal plane area 5.9% greater than PPL, and with a commensurate lowering of the density; the chain packing is similar but with a smaller chain setting angle. The

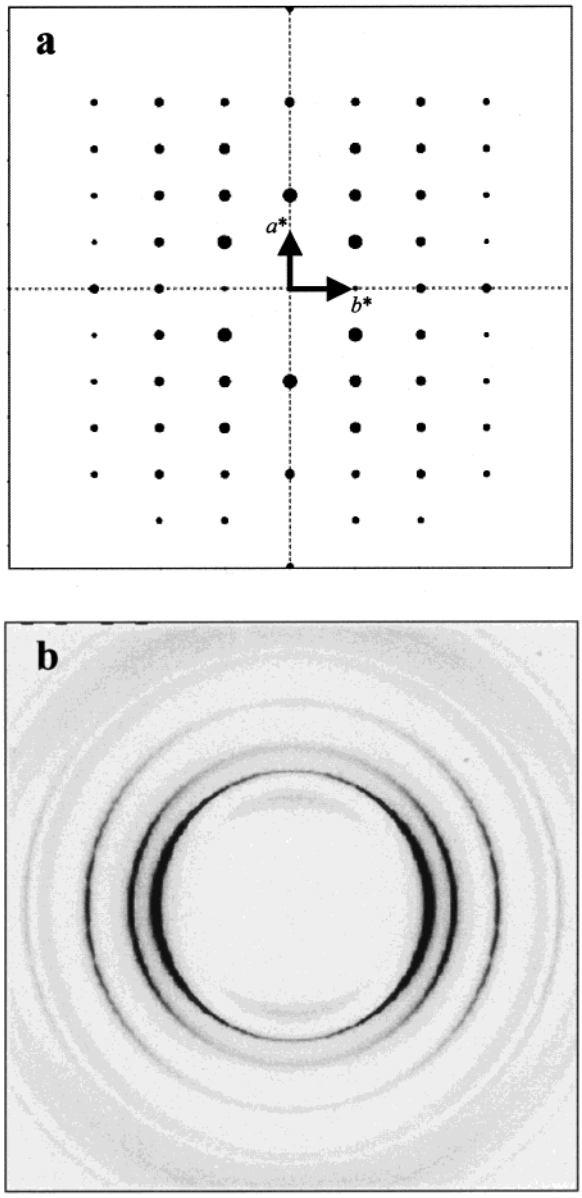

Figure 7. (a) Computer-simulated *hk*0 electron diffraction from the whole chain-folded PPL lamellar crystal, i.e., complete with folds. In the presentation of the simulated pattern the peak height value is expressed in terms of the area of the spot. It should be compared with the experimental pattern shown in Figure 2c. (b) Computer-simulated wide-angle X-ray diffraction pattern of PPL oriented mats; coincident *c*,*c** axes vertical. It should be compared with Figure 5a.

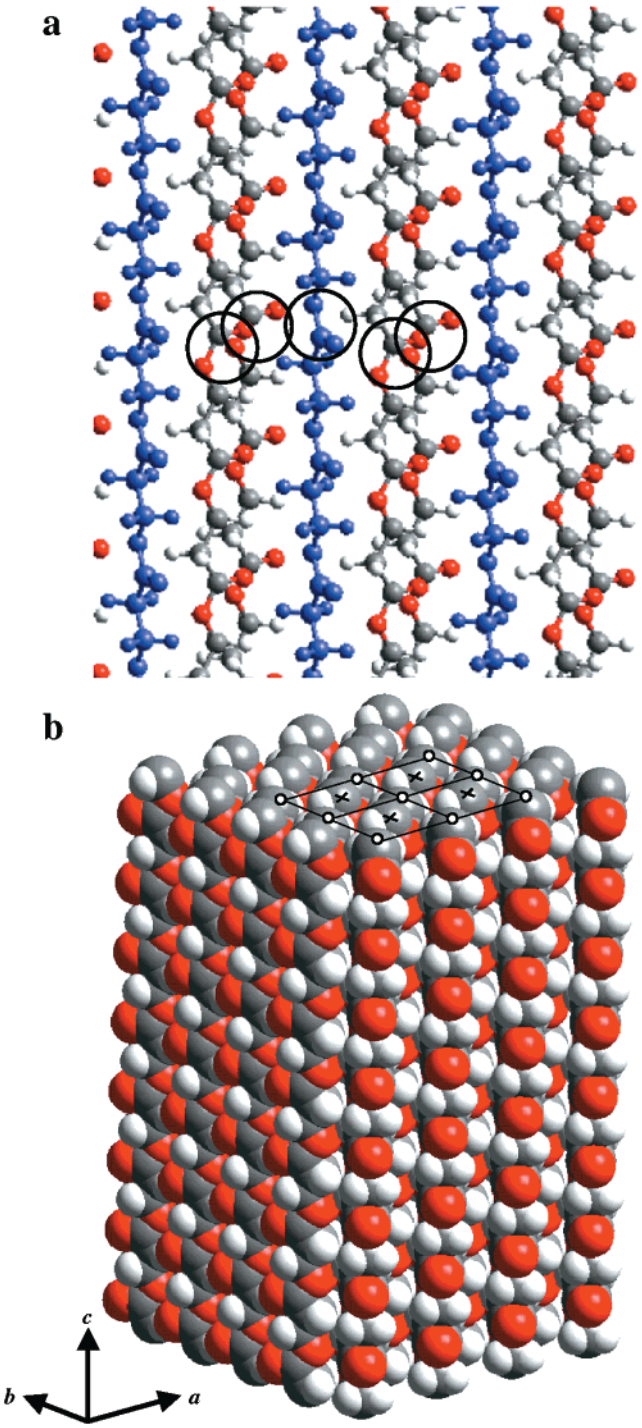

Figure 8. (a) Computer-generated ball-and-stick view of the PPL structure showing the relative displacement of ester groups between antiparallel chains: open circles. (b) Oblique view of straight-stem crystal in space-filling mode. The boxes represent the unit cell and the circles and crosses represent the ends of up and down straight-stems.

PE chains fold in a fashion similar to that for PPL; the rippling nature of the chain-folded sheets in PPL (see Figure 10) bear a strong resemblance to PE. As shown in Figure 9a, the ester groups in PPL are localized and this puts constraints on the relative *c*-axis displacement between the antiparallel chains; no such constraints exist in PE chain-folded lamellae. It is known that in PE chain-folded lamellar crystals, the chain-folded sheets often *c*-axis shear slightly to form sectorized pyramidal-shaped crystals;[18,20,21] i.e., the slight chain-folded sheet *c*-axis shear within a sector is similar to what we notice in our PPL lamellar crystals.

Comparison with P(3HB). This polyester may be thought of as a modification of PPL; a hydrogen atom on the carbon atom adjacent to the backbone oxygen being replaced with a methyl group. Thus, P(3HB) is PPL with an implanted $-CH_3$ side group. Inserting this methyl side group into an all-trans backbone is not possible owing to severe localized stereochemical clashing. As a consequence, two torsional angles associated with the dimethylene segments rotate from trans (T) to gauche (G) to relieve interatomic congestion resulting in a contracted 2-fold helix conformation, the axially projected monomer repeat dropping by 40%, from 0.493 to 0.298 nm.[9] The unit cell base (*ab* plane) is C-centered, and the chains in chain-folded lamellae the P(3HB)[17] follow the same pattern as for PPL.

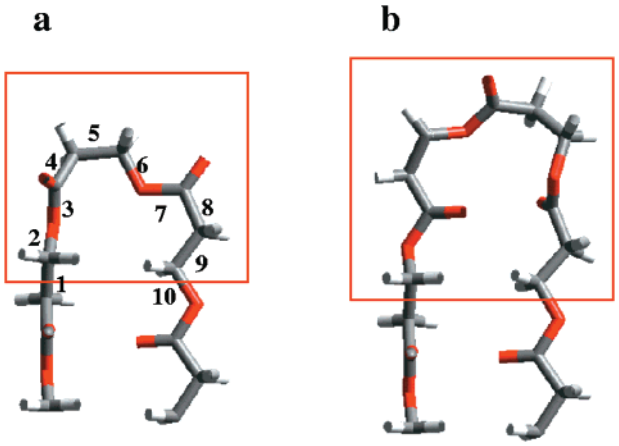

Figure 9. Views of the fold geometry: (a) the best fold with the dimethylene alkane segment close to the center of the hairpin turn (see Table 2b for torsion angle values of numbered bonds); (b) the less satisfactory fold with an ester group close to the center.

Comparison with Nylons. There is considerable similarity between PPL and the nylons,[22] the ester unit replacing the amide unit, with relatively short connecting dimethylene alkane segments. The inherent resistance to torsional rotation from the trans-conformation, about the O−CO ester bond in PPL, is analogous to the planar HN−CO amide unit in nylons. Of course, the dipole−dipole interactions in the polyesters are not as strong as those in the nylons, where they are expressed as hydrogen bonds. However, the nylons chain-fold into flat, rather than rippled, sheets, and the sheets stack together via van der Waals interactions. The lathlike morphology of PPL is similar to that observed in the nylons. In addition both twinning and *c*-axis shear[23] occur in chain-fold nylon lamellar crystals similar to that shown for PPL in Figure 3.

Conclusions

Chain-folded, lamellar crystals of poly-β-propiolactone (PPL), grown from cyclohexanone solution and isothermally crystallized, exhibit a lathlike morphology, 5 nm in thickness, and the chains run orthogonal to the lamellar surface. The average fold direction is along the *a* axis (long axis of the crystal) and the chain folds successively in the diagonal (110) and ($1\bar{1}0$) planes. There is evidence for slight *c*-axis shearing of the *chain-folded sheets*, along the lines previously discovered in sectorized pyramidal-shaped polyethylene crystals. We envision that during growth the chains extend into solution in the average direction of the long axis (*a* axis) of the chain-folded crystal. The evidence is consistent with regular, adjacent re-entry folding.

We have discovered a new crystalline structure: the γ-structure, for PPL chain-folded lamellar crystals. Nonfolded oligomers also exhibit the same unit cell; thus, it is unlikely to be a consequence of the chain-folding. The chain is in an all-trans or 1-fold helix conformation and crystallizes in a two-chain, C-faced, orthorhombic unit cell with the following parameters:

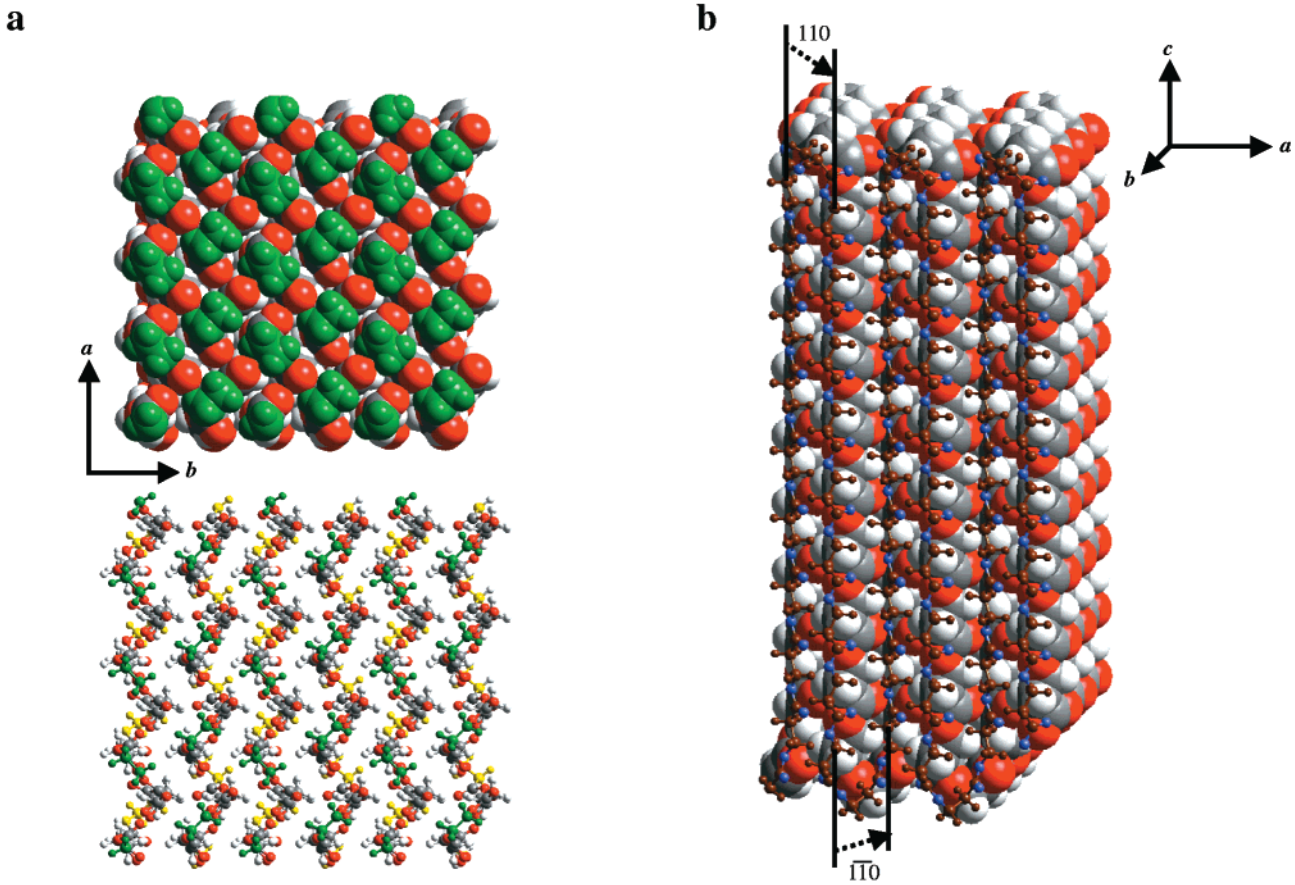

Figure 10. Views of the chain-folded lamellar crystal. (a) On the top, a view of the space-filling model parallel to the *c* axis showing the arrangement of folds along the ($1\bar{1}0$) planes; on the bottom, a similar view in ball-and-stick mode. In this latter view the folds along the (110) planes at the bottom of the chain-folded crystal can also be seen. (b) Oblique view of the space-filling model for the final structure. The front layer shows a single chain in ball-and-stick mode to illustrate the chain folding behavior within the crystal.

$a = 0.700 \pm 0.002$ nm, $b = 0.490 \pm 0.002$ nm, and c (chain axis) $= 0.493 \pm 0.002$ nm. The setting angles, with respect to the a axis, are $\pm 51.5°$ for the corner and center chains, respectively, and the relatively high density of 1.42 g cm^{-3} imposes severe restrictions on these values.

Detailed structure refinement shows that the ester units are in close proximity within the straight-stem core. The favored adjacent re-entry folds have the relatively short dimethylene segment close to the fold apex.

Acknowledgment. The authors thank Dr. H. Nishida of Tsukuba Research Laboratory, Tokuyama Corporation for providing the samples used in this study. Y.F. is a recipient of the Special Postdoctoral Researchers Program of the RIKEN Institute. E.A. wishes to thank the RIKEN Institute (International Cooperation Office) for a Visiting Eminent Scientist Award and the Engineering and Physical Research Council for support. P.S. is a recipient of a University of Bristol and Overseas Research Council Ph.D Scholarship. This work has been supported by CREST (Core Research for Evolutional Science and Technology) of the Japan Science and Technology Corporation (JST).

References and Notes

(1) Doi, Y. *Microbial Polyesters*; VCH Publishers: New York, 1990.
(2) Anderson, A. J.; Dawes, E. A. *Microbiol. Rev.* **1990**, *54*, 450. Dawes, E. A.; Senior, P. J. *Adv. Microb. Physiol.* **1973**, *10*, 135.
(3) Abe, H.; Doi, Y.; Aoki, H.; Akehata, T. *Macromolecules* **1998**, *31*, 1791.
(4) Iwata, T.; Doi, Y.; Kasuya, K.; Inoue, Y. *Macromolecules* **1997**, *30*, 833.
(5) Iwata, T.; Doi, Y.; Tanaka, T.; Akehata, T.; Shiromo, M.; Teramachi, S. *Macromolecules* **1997**, *30*, 5290.
(6) Iwata, T.; Doi, Y. *Macromol. Chem. Phys.* **1999**, *200*, 2429.
(7) Wasai, T.; Saegusa, T.; Furukawa, J. *Chem. Soc. Jpn., Ind. Chem. Sect.* **1964**, *67*, 601.
(8) Suehiro, K.; Chatani, Y.; Tadokoro, H. *Polym. J.* **1974**, *7*, 352.
(9) Yokouchi, M.; Chatani, Y.; Tadakoro, H.; Teranishi, K.; Tani, H. *Polymer* **1974**, *14*, 267.
(10) Okamura, K.; Marchessault, R. H. In *Conformation of Biopolymers*; Ramachandran, G. N., Ed.; Academic Press: New York, 1967; Vol. 2, pp 709−720.
(11) Okamura, K. *Kobunshi* **1972**, *21*, 525.
(12) Wittmann, J. C.; Lotz, B. *J. Polym. Sci., Polym. Phys.* **1985**, *23*, 205.
(13) Girolamo, M.; Keller, A.; Stejny, J. *Makromol. Chem.* **1975**, *176*, 1489.
(14) Model building calculations and X-ray diffraction results agree on a c-axis periodicity of 0.493 ± 0.002 nm; this differs slightly (3%) from that originally reported by Suehiro et al.[8] in 1974.
(15) The calculation was performed on the complete chain-folded crystal as shown later in Figure 10; i.e. it incorporated the folds. In testing for the goodness in fit, the computer matches the peak heights of the spot pattern; however, in the presentation of the simulated pattern, the peak height value is expressed in terms of the area of the spot.
(16) The diffraction arises from a whole lamella, or a one-dimensional stack in the case of the X-ray diffraction pattern; thus, the molecular transform is sampled at other regions of reciprocal space, other than at *hkl* reciprocal lattice points.
(17) Bireley, C.; Briddon, J.; Sykes, K. E.; Barker, P. A.; Organ, S. J.; Barham, P. J. *J. Mater. Sci.* **1995**, *30*, 633.
(18) Geil, P. H. *Polymer Single Crystals*; Interscience: New York, 1963.
(19) Bunn, C. W. *Trans. Faraday Soc.* **1939**, *35*, 482.
(20) Keller, A. *Prog. Phys.* **1968**, *31*, 41.
(21) Reneker, D. H.; Geil, P. H. *J. Appl. Phys.* **1960**, *31*, 1916.
(22) Jones, N. A.; Atkins, E. D. T.; Hill, M. J. *Macromolecules* **2000**, *33*, 2642.
(23) Bermudez, M.; Leon, S.; Aleman, C.; Munoz-Guerra, S. *J. Polym. Sci., Polym. Phys.* **2000**, *38*, 41.

MA001070T